BMC Musculoskeletal Disorders

RESEARCH

Open Access

Articular cartilage degeneration and aberrant osteocyte perilacunar/canalicular remodeling in subchondral bone of patients with developmental dysplasia of the hip

Teng Ye[1†], Jiren Yan[1†], Tianyou Kan[2,3†], Guoming Xie[1], Zhichang Zhang[1], Wenjing Yin[1], Bizeng Zhao[1], Zhifeng Yu[2*] and Linyang Chu[1*]

Abstract

Background Developmental dysplasia of the hip (DDH) is a congenital musculoskeletal disease that impairs the hip joint and exacerbates hip osteoarthritis. This study aims to investigate the alterations of osteocytic characteristics including apoptosis, lacuna-canalicular network, and perilacunar/canalicular remodeling (PLR) activity in subchondral bone from DDH patients, and potential relationship of these alterations between the cartilage degeneration and DDH progression.

Methods The femoral head specimens were acquired from 16 patients with hip fractures who received total hip arthroplasty operation, 24 patients with primary hip OA and 25 patients with DDH. The femoral head were scanned by a micro-computed tomography and the volume of interest was used for a micro-finite element analysis. Histological and immunohistochemical staining was used to observe chondrocytes in cartilage and osteocytes in subchondral bone. Terminal deoxynucleotidyl transferase dUTP nick end labeling staining was used to investigate the apoptotic osteocytes in subchondral bone. Ploton silver staining was used to visualize lacunocanalicular network and picrosirius red staining was to visualize collagen fiber orientation in subchondral bone.

Results The DDH group showed the highest apoptosis rate of osteocytes and increased PLR activity among the three groups. The micro–finite-element analysis revealed that DDH group had deteriorative microstructural and biomechanical properties of subchondral bone. The histological and immunohistochemical analyses showed that the cartilage degeneration in DDH group was the most severe. Linear regression analysis revealed a significant correlation between osteocytic activity in subchondral bone and cartilage degeneration in DDH.

[†]Teng Ye, Jiren Yan and Tianyou Kan contributed equally to this work.

*Correspondence:
Zhifeng Yu
zfyu@outlook.com
Linyang Chu
chulinyang@alumni.sjtu.edu.cn

Full list of author information is available at the end of the article

Conclusions Our findings indicate that the abnormal osteocyte activity in subchondral bone might contribute to the deterioration of subchondral bone structure, which accelerates cartilage degeneration and DDH progression. Targeting subchondral bone remodeling could offer a promising therapeutic strategy for DDH.

Keywords Subchondral bone, Osteocyte, Biomechanics, Developmental dysplasia of the hip, Cartilage degeneration

Background

Developmental dysplasia of the hip (DDH) is a musculoskeletal disorder and impairs the joint function [1]. DDH can cause hip instability, resulting in inhomogeneous stress distribution, which can lead to secondary osteoarthritis (OA) and severe cartilage degeneration. The prevalence of DDH was 5–30 per 1000 in clinically screened populations and 1–2 per 1000 in unscreened populations, indicating that DDH has become a significant public health issue [2]. Most patients with DDH will evolve into severe hip OA in later stages and require total hip arthroplasty (THA) [3]. Given the large population of DDH patients, there is an urgent need for comprehensive treatment strategies.

Previous studies have indicated that subchondral bone plays a crucial role in the pathogenesis of primary OA [4–6], while its specific role in DDH remains poorly understood. Compared to articular cartilage, subchondral bone has relatively greater stiffness and biomechanical properties, enabling it to bear most of the mechanical forces transferred from the joint surface, thus providing biomechanical support to the overlying cartilage [7]. Moreover, the biomechanical and microstructural properties of subchondral bone could be altered by the mechanical forces acting on the joint. Moderate exercises could promote bone density in the weight-bearing bones, while long-term exposure to microgravity environment could result in a bone loss of 1–1.5% in bone mineral density [8]. Because of the abnormal articular structure in patients with DDH, femoral head undergoes a long-term luxation tendency as well as the aberrant biomechanical condition, which would inevitably cause severe damage to the microstructural and biomechanical properties of subchondral bone. This abnormal loading is a key factor contributing to the deterioration of the microstructural and biomechanical properties of the subchondral bone, a process that is not observed in primary OA to the same extent. Our previous clinical and animal studies have both demonstrated that DDH individuals had worse microstructures and poorer biomechanical properties of subchondral trabecular bone, which were associated with the cartilage degeneration. Moreover, the changes in subchondral bone in DDH occur earlier than articular cartilage degeneration, which is in contrast to OA, where cartilage degeneration often precedes changes in the subchondral bone. These subchondral changes in DDH were proved to result from abnormal bone remodeling [9, 10]. However, the specific cellular mechanisms underlying these alternations in subchondral bone from DDH patients remains unclear.

Recent studies have demonstrated that osteocytes, which constitute 85–90% cells of all adult bone, play a vital role in bone homeostasis and remodeling. These versatile cells can sense mechanical force by their dendrites and cell bodies and regulate orchestrate skeletal remodeling through secreting endocrine proteins in autocrine and paracrine manners [11, 12]. One of the distinct characteristics of osteocytes is that they form central small chambers (lacunae) and surrounding fluid-filled pipes (canaliculi), which collectively shape into lacuna-canalicular network (LCN) [13]. During mechanical loading, the fluid shear stress within the LCN is primarily sensed by osteocytes, thereby activating or suppressing the inherent perilacunar/canalicular remodeling (PLR) of osteocytes. During the dynamic process of PLR, osteocytes secret cathepsin K [14], matrix metalloproteinases (MMPs) [15], and other enzymes to directly resorb and remodel their surrounding bone matrix as well as LCN [16]. Moreover, previous reports have showed that the increased osteocyte apoptosis could be responsible for the abnormalities in perilacunar bone resorption and canalicular arrangement, which impairs the biomechanical properties [15, 17]. Given the unique and important functions of osteocytes, emerging studies have gradually unraveled their roles in various musculoskeletal diseases for the past few years, including OA [18], bone loss during lactation [14], and X-linked hypophosphatemia [19]. However, the characteristics of osteocytes and their relationship with subchondral bone remodeling, microstructural and biomechanical properties, and cartilage degeneration in DDH patients remain unclear.

Because abnormalities in the homeostasis of osteocyte activities could contribute to bone quality [15], our current studies were undertaken to elucidate osteocyte characteristics in clinical specimens from DDH patients. We investigated the relationship among the osteocyte apoptosis, LCN organization, PLR enzyme expression, subchondral bone microstructural/biomechanical properties, and cartilage degeneration. We hypothesize that abnormal osteocyte remodeling activity, caused by aberrant mechanical distribution in DDH patients, leads to the worsening of microstructure and biomechanical properties in subchondral bone, thereby accelerating cartilage degeneration, a process that differs mechanistically from OA, where osteocyte activity is

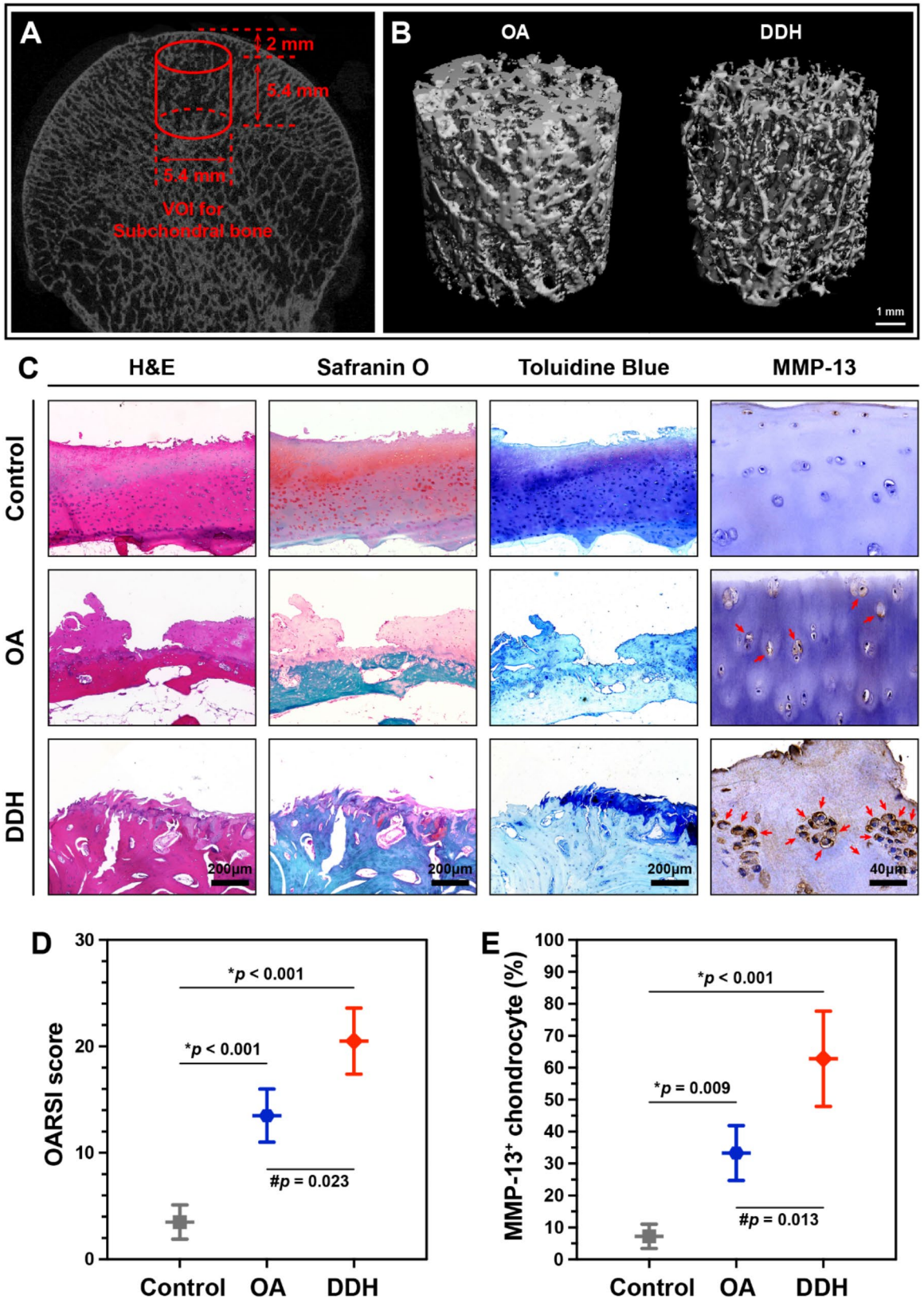

Fig. 1 (See legend on next page.)

(See figure on previous page.)

Fig. 1 Representative Micro-CT images of the femoral head specimens and the results of cartilage degeneration in the control, OA, and DDH groups. (**A**) VOI for subchondral bone (red dashed line) in the primary stress-bearing region of femoral head. (**B**) Reconstructed 3D image of the VOI area in subchondral bone in the OA and DDH groups, scale bar: 1 mm. (**C**) Representative images of histological staining and immunohistochemical staining for MMP-13 in each group (red arrows indicating the MMP-13^{+} chondrocytes). (**D**) Results of the Osteoarthritis Research Society International (OARSI) scoring system in each group. (**E**) Quantitative analysis for the MMP-13 positive chondrocytes in each group. *p <.05 compared with control group, #p <.05 compared with OA group

primarily influenced by long-term cartilage wear and mechanical overload [20].

Methods

Human subjects

The femoral head specimens were acquired from 24 patients with primary hip OA (OA group, 69.56 ± 11.47 years) and 25 patients with DDH (DDH group, 62.18 ± 13.62 years). The patients who were diagnosed as suffering primary hip OA or DDH underwent THA operation at Shanghai Ninth People's Hospital. Besides, 16 femoral head specimens from patients with the hip fractures who received THA operation were classified into the normal control group (Control group, 65.82 ± 8.31 years). The written informed consent was provided by all patients before their involvement into study. The patients got a physical examination and biochemical marker examination, to rule out those with systematic disorders (e.g., hematological diseases, endocrine disorders, liver or kidney metabolic diseases) which could influence the metabolism of bone. This study was approved by the Institute Review Board (IRB) of Shanghai Ninth People's Hospital (Reference number: 2018-179-T137). The femoral head specimens of different groups were collected for the following studies.

Micro-computed tomography analysis (μCT analysis)

The femoral head from different groups were analyzed by a micro-computed tomography system of high-resolution (Micro-CT 80; Scanco Medical AG, Switzerland) with an isotropic voxel size of 18 μm. The trabecula has particular patterns and could be corresponding to the region of compression and tension in the stressed central area of the femoral head [21]. The primary area perpendicular to the articular surface is suitable for observing bone alternations because it can respond to the transmitted loading stress from the joint face. Besides, the cylinder axis of the primary stress-bearing region is aligned with the main trabecular direction, which means the alternations of biomechanical properties based on the examining direction could be minimized [22]. According to the existed concept, virtual cylindrical biopsies (2 mm from the articular surface, Ø 5.4 mm, length 5.4 mm) determined by the semiautomatic contouring method as the volume of interest (VOI) in the primary stress-bearing region were calculated from the 3D reconstruction image (VOI for subchondral bone, as shown in Fig. 1A-B). A μCT system software (Scanco Medical AG, Image Processing Language Version 4.29d, Switzerland) was applied to calculate the microstructural properties of VOI. The total bone volume fraction (BV/TV), trabecular bone number (Tb.N), trabecular bone separation (Tb.Sp), and trabecular bone thickness (Tb.Th) were processed and acquired. The connectivity density (Conn.D) was characterized as a topological parameter of total bone trabecular connections per cubic millimeter. Also, the structure model index (SMI) was calculated by a model on the basis of the structure type.

Micro-finite element analysis (μFEA)

For μFEA, the axial compression tests for each subchondral bone cube in the longitudinal directions was performed by the Scanco Medical Finite Element Software 1.06 (Scanco Medical AG, Switzerland). The subchondral bone VOI was modeled to be homogeneous linear isotropic elastic material with a Poisson's ratio of 0.3 and a 15 GPa Young's modulus (Es) [23]. Afterwards, the uniaxial compression tests were adopted to analyze the reaction force while the axial translocation was equal to 1% of the bone segment height. Moreover, biomechanical properties including failure load and stiffness were automatically obtained from the μFEA.

Histological analysis

All groups specimens of selected VOI were used for following histological analysis. For the evaluation of cartilage, briefly, 5 μm serial sections were stained with HE, Safranin O-Fast Green, and Toluidine blue. The level of cartilage degeneration was measured by the Osteoarthritis research Society international scoring system (OARSI score). For the evaluation of osteocytes in subchondral bone, 5 μm serial sections were stained with HE, and the quantification of empty lacunae was performed by Image-pro Plus Software. Five sequential sections from each sample were processed and then analyzed.

Immunohistochemical analysis

Sections were processed for immunohistochemical analysis after μCT scanning. For the evaluation of chondrocytes in cartilage, sections were treated metalloproteinase-13 (MMP-13, Abcam, UK) primary antibody at 4℃ overnight. Then, sections were incubated with HRP-labelled secondary antibody at room

temperature for 1 h. The substrate color was generated using diaminobenzidine. For the analysis of osteocytes in subchondral bone, briefly, sections were processed as mentioned above and respectively incubated with caspase-3 (Abcam, UK), MMP-13 (Abcam, UK), and cathepsin K (Abcam, UK) primary antibodies. Next, HRP-labelled secondary antibody was incubated with the sections and diaminobenzidine was used for the development of substrate color. The images were obtained using an microscope (Leica Microsystems AG, Germany). Then, Image-pro Plus Software was adopted to calculate the number of positively stained cells. Additionally, five sequential sections from each specimen were processed and evaluated.

Terminal deoxynucleotidyl transferase dUTP nick end labeling (TUNEL) staining

To investigate the apoptotic osteocytes in subchondral bone, the sections were processed using the In Situ Cell Death Detection Kit, Fluorescein (Sigma-Aldrich). Images were obtained by fluorescent microscopy. Image-pro Plus Software was adopted to calculate the positively stained cells.

Ploton silver staining and Picrosirius red staining

As previously reported, the sections were incubated in two parts 50% silver nitrate and one part 1% formic acid in 2% gelatin solution for fifty-five minutes to visualize lacunocanalicular network [24]. The 5% sodium thiosulfate was used to wash stained slides for ten minutes and then dehydrated, cleared, and mounted. Images were captured at 100x magnification (OLYMPUS, IX71). The quantification of the lacunocanalicular area and the canalicular length was processed by Image-pro Plus Software.

For the visualization of collagen fiber orientation in subchondral bone, sections were incubated with a saturated aqueous solution of picric acid with 0.1% Direct Red-80 according to previous study [25]. Then, polarized light microscopy was used to obtain images. The OrientationJ plugin in ImageJ was adopted to extract Red channel images as described before [26].

Table 1 Basic information for the control, OA, and DDH groups

Characteristic	Control	OA	DDH	OA vs. DDH (*p* value)
N	16	24	25	
Gender (female/male), N	8/8	14/10	16/9	
Age (years)	65.82 ± 8.31	69.56 ± 11.47	62.18 ± 13.62	0.041*
Height (cm)	168.54 ± 6.42	164.89 ± 5.18	159.33 ± 7.45[b]	0.024*
Weight (kg)	68.31 ± 7.95	65.24 ± 6.77	59.48 ± 8.12[b]	0.017*
BMI (kg/m^2)	23.65 ± 4.33	24.36 ± 3.62	22.41 ± 2.75	0.347
Femur BMD (T value)	-1.12 ± 0.57	-0.63 ± 0.42[a]	-0.72 ± 0.48	0.261
Spine BMD (T value)	-1.38 ± 0.76	-0.48 ± 0.57[a]	-0.68 ± 0.94[b]	0.097
Alcohol use (%)	37.5	41.7	28	
Current smokers (%)	37.5	33.3	20	
Other systemic diseases	No	No	No	

Values represent mean ± SD; OA, osteoarthritis; DDH, developmental dysplasia of the hip; BMI, body mass index; BMD, bone mineral density. *p <.05 between OA and DDH group; [a]p <.05 between OA and control group; [b]p <.05 between DDH and control group

Statistical analysis

Data were analyzed by the SPSS Statistics v22 (IBM, Armonk, NY, USA) and presented as mean ± standard deviations (SDs). The data normality had been tested and verified for all variables by the Shapiro-Wilk test. One-way analysis of variance (ANOVA) with Tukey's post-hoc test was used for normally distributed parameters including age, height, weight, cartilage degeneration, subchondral bone microstructural and biomechanical properties, as well as osteocyte characteristics among the control, OA, and DDH groups. For the analysis of cartilage, subchondral bone and osteocyte characteristics, if the results were statistically significant, the parameters were compared again after adjusting for each potential covariate by the generalizing multiple linear regression analysis. Sets of covariates independent from each other were selected, including the age, height, and weight. Furthermore, to investigate relationship between cartilage, subchondral bone, and osteocytic characteristics, Pearson's correlation coefficient and linear regression analyses with osteocytic characteristics were applied for microstructural and biomechanical properties of subchondral bone as well as the OARSI score and the MMP-13 positive chondrocytes percentage. For all analyses, statistical significance was defined as a two-tailed p <.05.

Results

Basic clinical information

This study included 24 primary hip OA patients and 25 DDH patients, and 16 patients with the fractured femoral neck regarded as the control group. The detailed basic information is shown in Table 1. Patients with OA underwent THA operation were at an older age than patients with DDH (p <.05). Besides, DDH patients showed no differences with OA patients in body mass index (BMI), femur BMD and spine BMD (p >.05).

Analysis of cartilage degeneration

Histological and immunohistochemical analyses were applied to evaluate the cartilage degeneration

in all groups, the results are presented in Fig. 1C-E. The cartilage degeneration in DDH group was more severe than other groups, characterized by the damage of cartilage surface and destruction of proteoglycan (Fig. 1C). The result of OARSI score system revealed that the DDH group possessed the most severe cartilage degeneration among all groups (Fig. 1D, $p<.05$). From the immunohistochemical analysis, the percentage of MMP-13 positive chondrocytes in the DDH group was higher than other groups (Fig. 1C and E).

Analysis of subchondral bone microstructural and biomechanical properties

The microstructural properties of subchondral bone (subchondral trabecular bone in VOI of primary stress-bearing area) were analyzed by μCT, and the results are presented in Table 2. Obviously, the BV/TV and Conn.D were the lowest in the DDH group while OA group had the highest bone density and volume ($p<.05$). The DDH group had the highest Tb.Sp as well as the lowest Tb.N and Tb.Th ($p<.05$), which implied that patients with DDH had more incompact and deteriorated subchondral bone microstructure. Besides, the SMI value in DDH group significantly increased while compared with other groups, indicating that there were more rod-like trabecular bone rather than plate-like trabecular bone in DDH patients ($p<.05$). Additionally, μFEA analysis was performed to examine the biomechanical properties of subchondral bone in the control, OA, and DDH group. The results revealed that DDH group had the lowest stiffness and failure load properties among all groups ($p<.05$), while OA group had the highest biomechanical properties possibly because of the improved subchondral bone sclerosis ($p<.05$).

Analysis of osteocyte apoptosis in subchondral bone

The results of the histology, immunohistochemistry, and TUNEL staining for osteocyte apoptosis in the control, OA, and DDH groups are presented in Fig. 2. In the DDH group, the percentage of empty lacunae was significantly increased compared with other groups according to the H&E staining (Fig. 2A-B, $p<.05$). The results of TUNEL staining and immunohistochemical staining for caspase-3 revealed that the percentages of TUNEL positive and caspase-3 positive osteocytes were dramatically enhanced in the DDH group, indicating that the apoptosis rate of osteocytes in subchondral bone was elevated. Moreover, we have also observed that the apoptotic osteocyte rate of OA group fell in between the DDH group and control group (Fig. 2A and C-E, $p<.05$).

Analysis of collagen fiber organization, osteocyte lacunocanalicular network, and perilacunar/canalicular remodeling activity in subchondral bone

The collagen fiber organization could provide some clues to osteocytic action [16, 18]. Therefore, we observed the Picrosirius red-stained collagen fibers using polarized light microscopy in all groups. The results showed that subchondral bone of OA group was composed of more randomly arranged collagen fibers than control group (Fig. 3A-B), which was consistent with previous report [18]. Interestingly, we found that birefringent collagen fibers in subchondral bone from DDH group were even less aligned and with disorganized orientation than those from OA and control group, indicating serious aberrant osteocytic remodeling activities in patients with DDH (Fig. 3B).

To investigate one of the key hallmarks of perilacunar/canalicular remodeling (PLR) activity—the lacunocanalicular network (LCN), we performed Ploton Silver staining in all groups. The results revealed that subchondral bone from DDH group had both more

Table 2 Microstructural and biomechanical properties of subchondral bone for the control, OA, and DDH groups

	Control	OA	DDH	OA vs. DDH (*p* value)
Subchondral bone Microstructure (Micro-CT)				
BV/TV (%)	25.44 ± 6.58	37.27 ± 11.34[a]	19.16 ± 5.86[b]	< 0.001**
Tb.N (1/mm)	2.09 ± 0.43	2.76 ± 0.95[a]	1.58 ± 0.69[b]	0.005**
Tb.Th (mm)	0.19 ± 0.04	0.22 ± 0.06	0.15 ± 0.03	0.034*
Tb.Sp (mm)	0.55 ± 0.18	0.51 ± 0.26	0.79 ± 0.37[b]	0.028*
SMI	0.86 ± 0.41	0.73 ± 0.28[a]	1.89 ± 0.73[b]	< 0.001**
Conn.D ($1/mm^3$)	9.35 ± 3.11	14.68 ± 7.29[a]	6.82 ± 2.32[b]	0.013*
Subchondral bone Biomechanical Properties (μFEA)				
Stiffness (kN/mm)	5326.84 ± 2855.17	8263.29 ± 3795.73[a]	2681.23 ± 973.55[b]	< 0.001**
Failure Load (MPa)	192.28 ± 83.71	365.42 ± 201.89[a]	129.67 ± 48.53[b]	0.019*

Values represent mean ± SD; BV, bone volume; TV, total volume; Tb.N, trabecular bone number; Tb.Th, trabecular bone thickness; Tb.Sp, trabecular bone separation; SMI, structure model index; Conn.D, connectivity density

*$p<.05$, ** $p<.01$ between OA and DDH group and remained significant after adjustment for selected covariates

[a]$p < 0.05$ between OA and control group and remained significant after adjustment for selected covariates

[b]$p < 0.05$ between DDH and control group and remained significant after adjustment for selected covariates

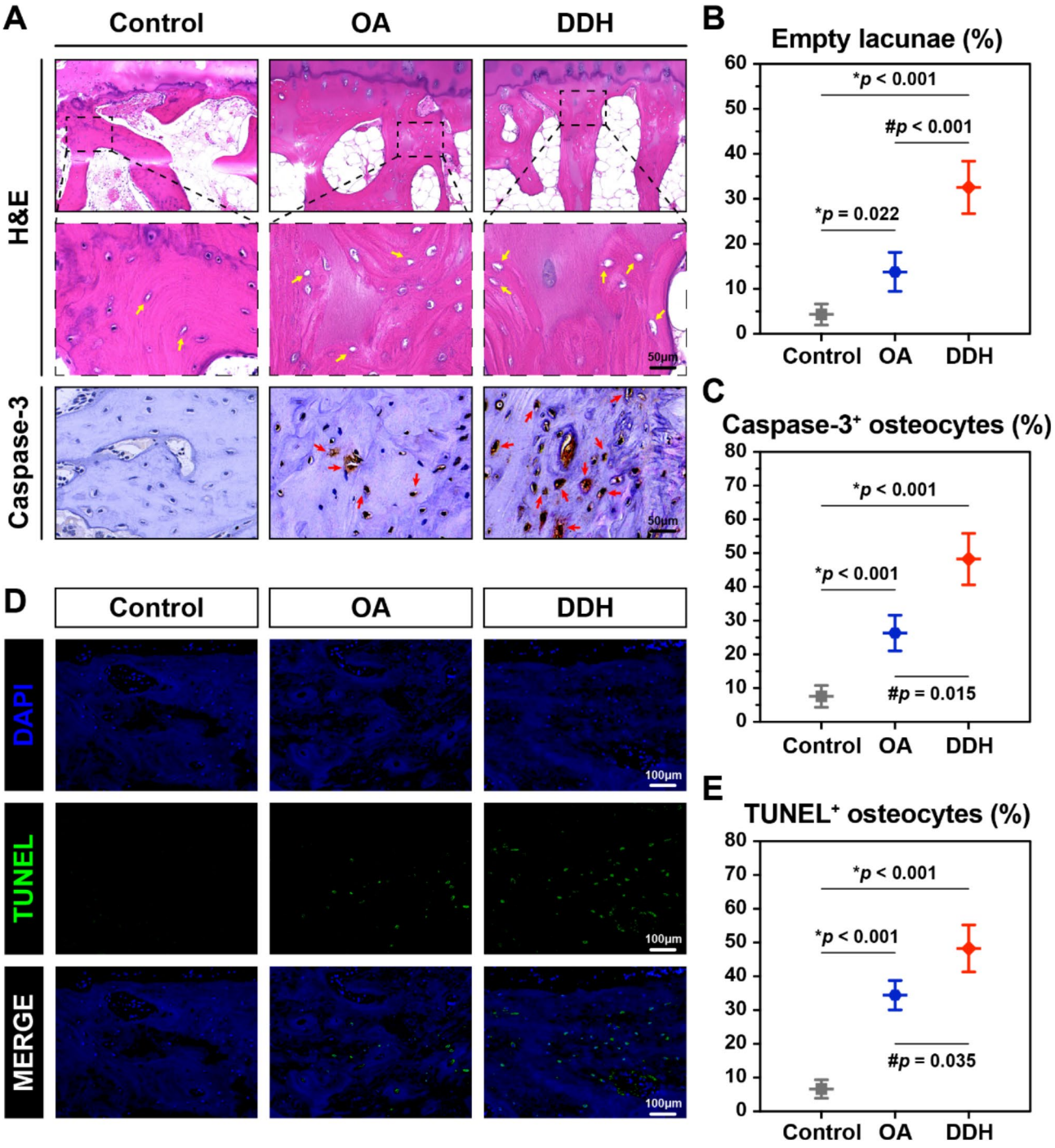

Fig. 2 The results of subchondral bone osteocyte apoptosis in the control, OA, and DDH groups. (**A**) Representative images of H&E staining (yellow arrows indicating empty lacunae, red arrows indicating the caspase-3$^+$ osteocytes) and immunohistochemical staining for caspase-3 in each group, scale bar: 100 μm. (**B**-**C**) Quantitative analysis for the percentage of empty lacunae and the percentage of Caspase-3 positive osteocytes in each group (**D**) Representative images of TUNEL staining in each group, scale bar: 100 μm. (**E**) Quantitative analysis for the percentage of TUNEL positive osteocytes in each group. *p <.05 compared with control group, #p <.05 compared with OA group

abundant and elongated canalicular projections than other groups (Fig. 3C). Also, the quantitative analysis showed significant increasement in the total osteocyte lacunocanalicular area and canalicular length in DDH group, while these properties were decreased in OA group (Fig. 3D-E, p <.05). Collectively, the enhanced lacunocanalicular area and canalicular length in DDH subchondral bone strongly implies that PLR is activated in DDH.

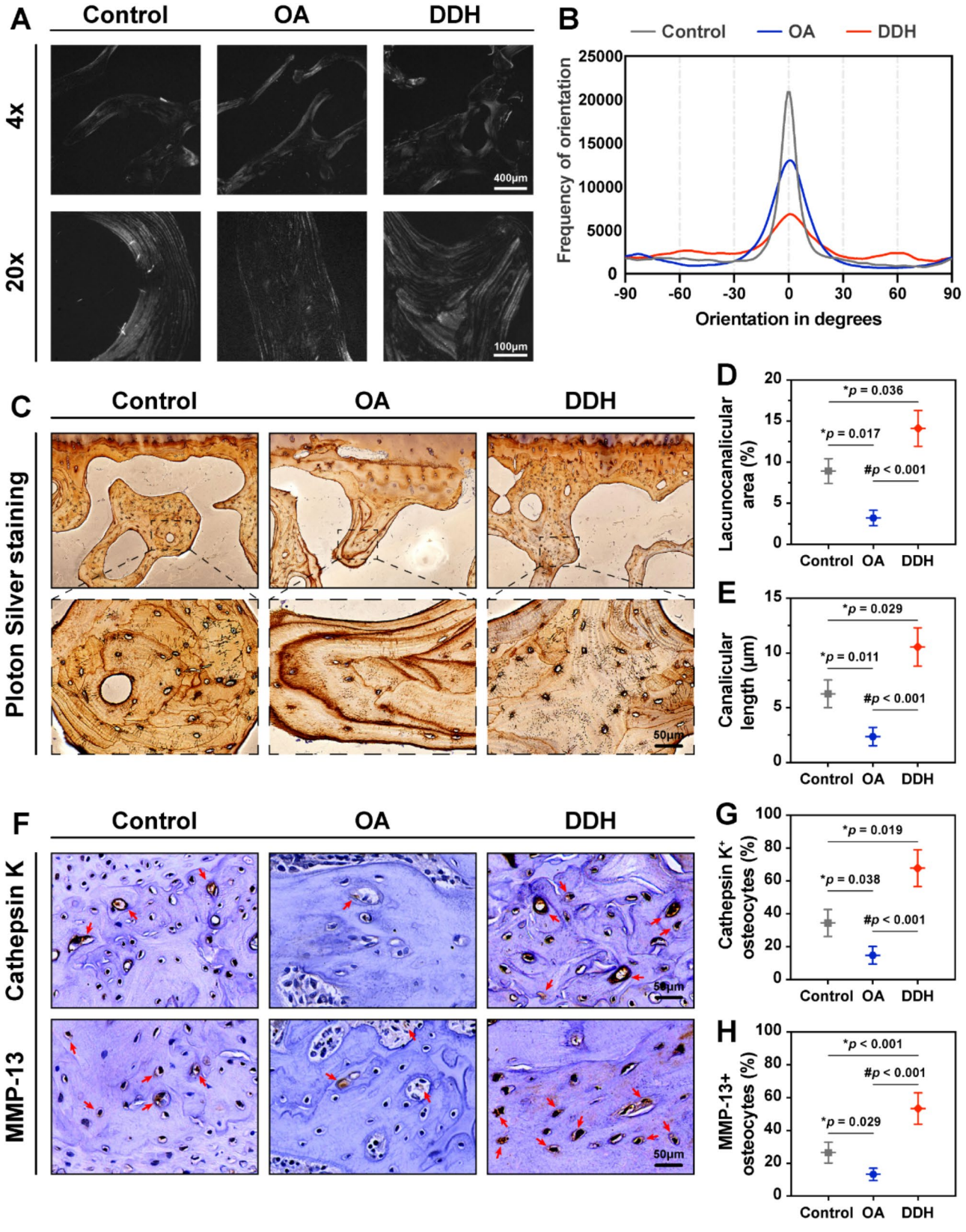

Fig. 3 (See legend on next page.)

(See figure on previous page.)

Fig. 3 The results of collagen fiber organization, lacunocanalicular network, and PLR enzyme expression in subchondral bone from the control, OA, and DDH groups. (**A**) Representative images of sections stained with Picrosirius Red and captured using polarized light microscopy at low (4x, top, scale bar: 400 μm) or high (20x, bottom, scale bar: 100 μm) magnification in each group. (**B**) The distribution of collagen fiber orientation shows differences between all three groups. (**C**) Representative images of Ploton Silver staining in each group, scale bar: 50 μm. (**D**-**E**) Quantitative analysis for the lacunocanalicular area normalized to bone area and the canalicular length in each group. (**F**) Representative images of immunohistochemical staining for PLR enzyme (including cathepsin K and MMP-13) in each group (red arrows indicating the cathepsin K^+ and MMP-13^+ osteocytes), scale bar: 100 μm. (**G**-**H**) Quantitative analysis for the percentage of cathepsin K positive and MMP-13 positive osteocytes in each group. *$p < .05$ compared with control group, #$p < .05$ compared with OA group

Given that subchondral bone from patients with DDH showed multiple features of activated PLR, we further examined the expression level of key enzymes involved with PLR. The results of immunohistochemical staining for cathepsin K and MMP-13 revealed qualitatively higher expression levels of these enzymes in subchondral bone from DDH group relative to other groups (Fig. 3F-H). In short, these results shows that DDH is highly associated with PLR activation, as proved by enhancement of lacunocanalicular area and canalicular length, as well as elevated levels of PLR enzymes in subchondral bone.

Linear regression analysis between osteocytic characteristics, subchondral bone properties, and cartilage degeneration

Linear regression analysis was employed to clarify the correlation between osteocytic characteristics and subchondral bone microstructural/biomechanical properties; shown in Table 3. The results revealed that the E. Lac, TUNEL, Cas-3, MMP-13 (O), LCN. A, and Can. L might be the key contributing factors in osteocytic characteristics for the subchondral bone microstructural properties in both DDH and OA groups ($r^2 > 0.3$, $p < .05$). In addition, the osteocytic characteristics showed a strong association with the subchondral bone biomechanical properties (SN and FL) in both groups ($r^2 > 0.3$, $p < .05$). Interestingly, the correlation between osteocytic characteristics and subchondral microstructural/biomechanical properties was more closer in the DDH group than in the OA group, due to the higher correlation coefficients. We also found that some osteocytic characteristics (E. Lac, TUNEL, and Cas-3) were positively correlated with the microstructural/biomechanical properties (BV/TV, Tb.N, Conn.D, Tb.Th, SN, and FL) in the OA group and negatively correlated with these microstructural/biomechanical properties in the DDH group, indicating that osteocytes probably played different roles between these two diseases. Furthermore, linear regression analysis was also adopted to investigate the relationship between osteocytic characteristics and cartilage degeneration (Table 4). The results revealed that while the osteocytic characteristics were highly correlated with the cartilage degeneration in both groups ($r^2 > 0.3$, $p < .05$), the correlation was even higher in the DDH group, suggesting that osteocytic activities played a more important part in cartilage damage in patients with DDH.

Discussion

In this study, the osteocytic characteristics in subchondral bone from DDH patients, including the apoptosis, collagen fiber organization, LCN, and PLR activity, were investigated for the first time. Our previous studies have revealed that the alternations of subchondral bone remodeling activity and biomechanical properties could play a crucial part in the cartilage degeneration as well as DDH progression [9]. Here, we found that the changes of osteocytic characteristics appeared to associate with the subchondral bone remodeling activity, which could contribute to the deteriorative microstructural and biomechanical properties as well as the overlying cartilage degeneration in DDH. This underscores the idea that subchondral bone remodeling, particularly osteocytic activity, is not merely a secondary effect, but a primary driver of the pathological changes observed in DDH. These findings broaden our knowledge of the crosstalk between subchondral bone and cartilage by involving osteocytes as a causal factor in DDH. Moreover, this study reveals increased osteocyte apoptosis and suggests PLR activation as a pivotal mechanism in DDH. Hence, osteocytes might be a promising cellular target for preventing or treating DDH progression.

Subchondral bone plays a crucial role in the progression of primary OA, and emerging studies have demonstrated the underlying cellular mechanism responsible for the abnormal sclerosis in subchondral bone [27–29]. However, little is known about these mechanisms in DDH. As mentioned before, our results for osteocytic apoptosis and PLR activity indicated that the osteocyte apoptosis was increased in both OA and DDH groups, while the PLR enzyme expression was decreased in OA group and increased in DDH group. This phenomenon is complex and somewhat controversial. Indeed, the opposite relevance between osteocyte apoptosis and PLR activity has been found in different musculoskeletal diseases according to previous studies. He et al. reported the increasing osteocyte apoptosis in a mouse osteoarthritis model and Mazur et al. found the suppressed osteocytic PLR activity in patients with osteoarthritis [18, 30], which were in line with our observations from OA group. In addition,

Table 3 Correlation coefficient of linear regression between osteocytic characteristics and subchondral bone properties

Parameter	E.Lac	TUNEL	Cas-3	CTSK	MMP-13(O)	LCN.A	Can.L
OA group							
BV/TV	0.37*	0.39*	0.43*	-0.26	-0.34*	-0.16	-0.35*
Tb.N	0.42*	0.34*	0.29	-0.22	-0.28	-0.32	-0.26
Tb.Th	0.28	0.04	-0.08	-0.07	-0.18	0.09	-0.21
Tb.Sp	-0.15	-0.23	-0.24	-0.19	-0.14	-0.36*	-0.11
SMI	-0.34*	-0.38*	-0.31	0.23	0.39*	0.44*	0.27
Conn.D	0.52*	0.37*	0.27	-0.33*	-0.36*	-0.29	-0.43*
SN	0.38*	0.27	0.34*	-0.15	-0.19	-0.28	-0.37*
FL	0.29	0.36*	0.24	-0.25	-0.23	-0.43*	-0.26
DDH group							
BV/TV	-0.58**	-0.48*	-0.61**	-0.49*	-0.53*	-0.38*	-0.65**
Tb.N	-0.55**	-0.52*	-0.57**	-0.39*	-0.66**	-0.37*	-0.43*
Tb.Th	-0.06	-0.16	-0.17	-0.29	-0.34*	0.13	-0.35*
Tb.Sp	0.24	0.29	0.33*	0.27	0.42*	0.31	0.26
SMI	0.43*	0.56**	0.48*	0.47*	0.41*	0.64**	0.59**
Conn.D	-0.62**	-0.44*	-0.38*	-0.63**	-0.59**	-0.45*	-0.61**
SN	-0.54*	-0.44*	-0.49*	-0.63**	-0.42*	-0.43*	-0.25
FL	-0.46*	-0.51*	-0.62**	-0.53*	-0.37*	-0.55**	-0.35*

E.Lac, empty lacunae; Cas-3, Caspase-3; CTSK, Cathepsin K; MMP-13(O), MMP-13 in osteocyte; LCN.A, lacunocanalicular area; Can.L, canalicular length; BV, bone volume; TV, total volume; Tb.N, trabecular bone number; Tb.Th, trabecular bone thickness; Tb.Sp, trabecular bone separation; SMI, structure model index; Conn.D, connectivity density; SN, stiffness; FL, failure load

*$p < .05$ and **$p < .001$ for correlation coefficient

Table 4 Correlation coefficient of linear regression between osteocytic characteristics and cartilage degeneration

Parameter	E.Lac	TUNEL	Cas-3	CTSK	MMP-13(O)	LCN.A	Can.L
OA group							
OARSI	0.33*	0.22	0.38*	-0.36*	-0.38*	-0.23	-0.39*
MMP-13(C)	0.19	0.35*	0.13	-0.34*	-0.17	-0.18	-0.11
DDH group							
OARSI	0.64**	0.58**	0.39*	0.48*	0.21	0.42*	0.56**
MMP-13(C)	0.31	0.37*	0.26	0.54**	0.35*	0.27	0.49*

E.Lac, empty lacunae; Cas-3, Caspase-3; CTSK, Cathepsin K; MMP-13(O), MMP-13 in osteocyte; LCN.A, lacunocanalicular area; Can.L, canalicular length; MMP-13(C), MMP-13 in chondrocyte

*$p < .05$ and **$p < .001$ for correlation coefficient

Tokarz et al. exhibited that long bones from mice with X-Linked Hypophosphatemia had increased osteocyte apoptosis, along with increased osteocyte mRNA and protein expression level of PLR key enzymes MMP-13 and cathepsin K [19]. Given the unique stress-sensing function of osteocytes, we hypothesize that the distinct mechanical environments and stress distributions between OA and DDH explain the different osteocytic properties in subchondral bone. In our previous study, we selected patients with OA and osteoporotic osteoarthritis (OP-OA) to compare the characteristics of articular cartilage and subchondral bone. We found that isolated OA primarily presents as cartilage degeneration and subchondral bone sclerosis, typically caused by the excessive concentration of mechanical load. In contrast, OP-OA is characterized by reduced subchondral bone density, leading to weakened bone structure and uneven cartilage load distribution. Our results suggest that the subchondral bone in DDH resembles that in OP-OA, and therefore DDH is likely to exhibit the same biological characteristics as OP-OA [29]. In DDH patients, the abnormal loading stress could activate the osteocytic activity and probably promote osteoclast formation, as the osteoclast activity was relatively more active in subchondral bone from DDH patients according to our recent research [9]. Besides, osteocytes utilize PLR to maintain the bone quality, partly by directly resorbing and replacing the local bone extracellular matrix [31, 32]. The PLR enzymes expression was elevated in the osteocytes as well as the increase of LCN area and canalicular length in the subchondral bone from DDH patients. These biological markers of osteocytic activity, such as increased PLR enzyme expression and expanded LCN area, are indicative of a pathological bone remodeling process in DDH that mirrors what is seen in osteoporotic conditions. These results strongly suggested that osteocytes in DDH group could cause bone resorption and inferior subchondral bone

microstructural/biomechanical properties by activated remodeling activity.

Emerging studies have concentrated on the crosstalk between cartilage chondrocytes and subchondral bone cells during the OA pathogenesis [33, 34]. Sanchez et al. found that chondrocytes co-cultured with osteoblasts from OA patients showed increased expression of catabolic genes and decreased expression of anabolic genes, compared to chondrocytes co-cultured with osteoblasts from normal bone [35]. Moreover, a recent study reported that circulating exosomal osteoclast-derived microRNAs could reduce the tolerance of cartilage to matrix degradation and thereby contributing to the OA progression, whereas blockage of osteoclast-originated exosomes slowed the process of OA [36]. Mature osteoblasts can directly regulate chondrocytes by enhancing osteoclast formation via interleukin-6 and prostaglandin E2, and indirectly by stimulating blood vessel formation and recruiting osteoclasts via vascular endothelial growth factor [37–41]. Similarly, exposure of osteocytes of subchondral bone to pro-inflammatory cytokines (e.g., interleukin-1β) released by OA chondrocytes upregulates the expression of osteoblastic VEGF and Receptor Activator of Nuclear Factor-κB Ligand, recruiting and activating osteoclasts, and exacerbating cartilage degradation [42, 43]. This highlights the potential paracrine role of osteocytes in DDH, where osteocytic activity might influence cartilage degradation in a manner similar to OA, but under different mechanical stresses. These evidences strongly suggest that the crosstalk may also exist between the osteocytes and chondrocytes in DDH, which means that abnormal osteocytic activities could account for the cartilage degeneration in a direct way. Indeed, our linear regression analysis also showed that the osteocytic characteristics were highly associated with the cartilage in DDH group. We infer that the activated osteocytic PLR activities in DDH subchondral bone could break the chondrocyte metabolic homeostasis in a paracrine pathway and cause cartilage degeneration, which needs to be further explored.

On the basis of present study and existing theories, we developed a model illuminating the changes of osteocytic characteristics of subchondral bone from DDH patients, and how these changes could contribute the cartilage degeneration (Fig. 4). So far, mounting evidence has clarified that mechanical loading stress could modulate the bone quality by regulating the interplay between bone remodeling cells including osteocytes [44–46]. Due to the aberrant hip joint structure, abnormal loading stress around femoral head could promote the abnormal osteocytic activity in the subchondral bone, subsequently leading to the inferior microstructural/biomechanical properties of subchondral bone. These alternations could decrease the loading stress transmitted from the cartilage layer to the subchondral bone and result in enhanced loading stress concentrated on the cartilage layer, thus promoting cartilage degeneration and DDH progression. Otherwise, the crosstalk between osteocytes and chondrocytes might be another reason for the severe cartilage damage, which needs further investigation.

Several shortcomings in this study need to be declared. First, the relatively small sample size may introduce selection bias. Second, this study is cross-sectional as our specimens were collected from patients with advanced hip OA and DDH. If possible, it should be better to observe the subchondral bone changes based on in vivo measurements. Fortunately, the second-generation high-resolution peripheral quantitative computed tomography is a hopeful candidate for the in vivo analysis [47]. Finally, though we proposed that the crosstalk between osteocytes and chondrocytes could play a crucial part in DDH progression, we didn't reveal any mechanisms related to this potential crosstalk in this study. Our further study aims to elucidate the potential causality and underlying mechanisms.

Conclusions

Collectively, our study indicates that patients with DDH have increased osteocyte apoptosis, less aligned collagen fiber organization, and activated osteocytic PLR activity. The abnormal osteocytic PLR activity in subchondral bone contribute to deteriorative subchondral bone microstructural and biomechanical properties along with serious cartilage degeneration that leads to exacerbated DDH progression. To the best of our knowledge, this is the first study to clarify the osteocytic characteristics in subchondral bone from DDH patients. These findings suggest osteocytes might be a hopeful cellular target for improving subchondral bone and contribute to preventing cartilage degeneration as well as alleviate DDH progression.

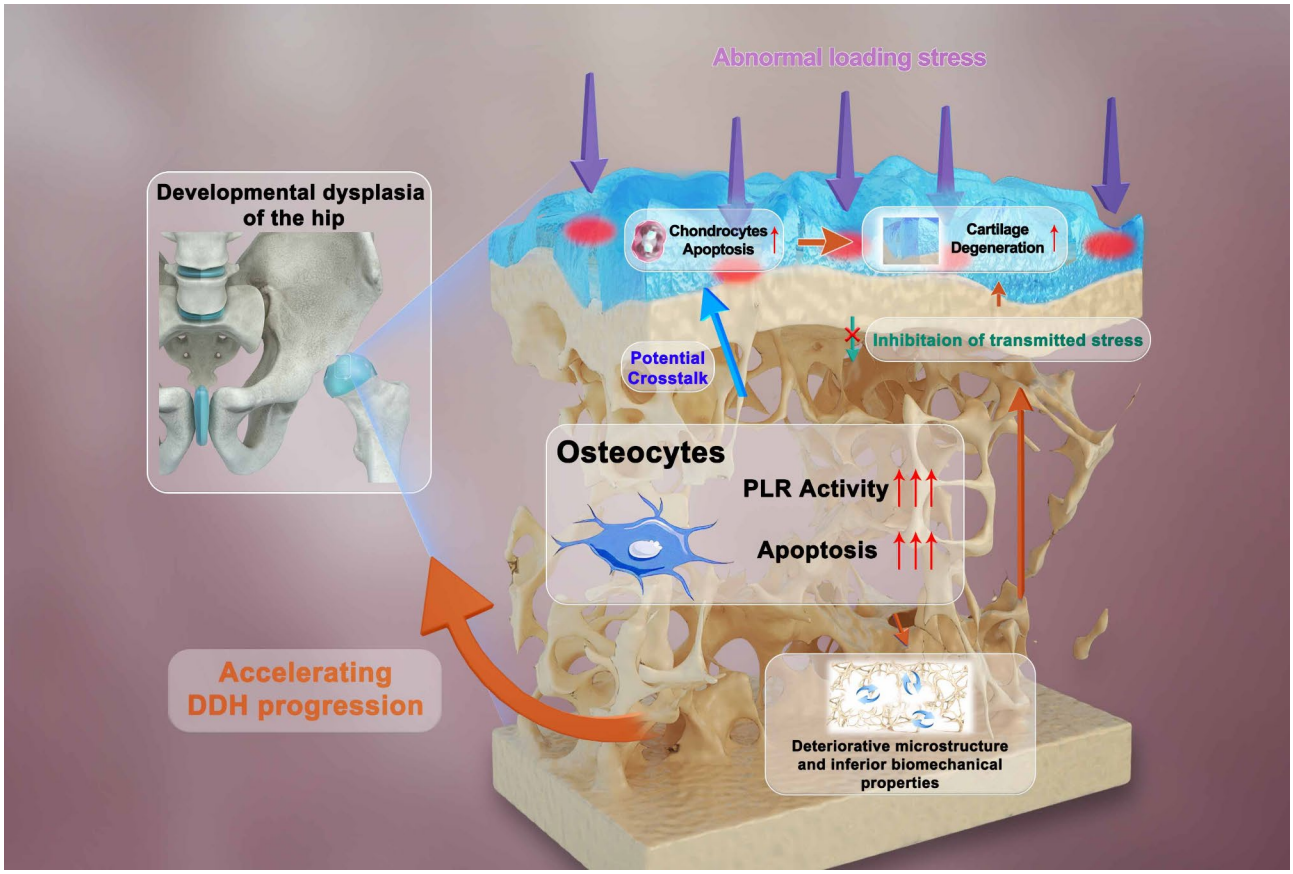

Fig. 4 Schematic diagram for the potential mechanism of abnormal osteocytic activity in the pathogenesis of DDH patients. The aberrant loading stress could lead to activated osteocytic PLR activity and increased osteocyte apoptosis in subchondral bone. The abnormal osteocytic activity in subchondral bone may account for the deteriorative microstructure and inferior biomechanical properties, which inhibits the transmitted loading stress from the cartilage layer to the subchondral bone, resulting in the enhanced loading stress focused on the cartilage layer and promoting the cartilage degeneration as well as DDH progression. Moreover, the potential crosstalk between osteocytes and chondrocytes may be another reason for the apoptosis of chondrocytes and cartilage degeneration

Abbreviations

DDH	Developmental dysplasia of the hip
OA	Osteoarthritis
THA	Total hip arthroplasty
LCN	Lacuna-canalicular network
MMPs	Matrix metalloproteinases
μCT	Micro-computed tomography
VOI	Volume of interest
BV/TV	Total bone volume fraction
Tb.N	Trabecular bone number
Tb.Sp	Trabecular bone separation
Tb.Th	Trabecular bone thickness
Conn.D	Connectivity density
SMI	Structure model index
μFEA	Micro-finite element analysis
OARSI	Osteoarthritis research Society international
TUNEL	Terminal deoxynucleotidyl transferase dUTP nick end labeling
SDs	Standard deviations
ANOVA	Analysis of variance
BMI	Body mass index

Acknowledgements
Not applicable.

Author contributions
TY, LC, BZ and ZY were involved in the study design, data collection and basic analysis of data. TY, JY and TK were involved in the statistical analysis and drafted the manuscript. GX, ZZ and WY contributed to data acquisition, interpretation, and experimental suggestions. LC, BZ and ZY provided funding to support the study. ZY and BZ contributed to the manuscript revising. All the authors have read and approved the submitted manuscript.

Funding
This work was sponsored by the Youth Program of National Natural Science Foundation of China (No. 32000926), Shanghai Sailing Program (No. 20YF1435600), the National Natural Science Foundation of China (No. 81870972), and the Natural Science Foundation of Shanghai (No.20ZR1432000).

Data availability
The datasets generated and/or analyzed during the current study are available from the corresponding author by reasonable request.

Declarations

Ethics approval and consent to participate
This study was approved by the Institute Review Board (IRB) of Shanghai Ninth People's Hospital (Reference number: 2018-179-T137). The guidelines of human ethics according to the Declaration of Helsinki were followed. All participants signed and written informed consent.

Consent for publication
Not applicable.

Competing interests
The authors declare no competing interests.

Author details
[1]Department of Sports Medicine, National Center for Orthopaedics, Shanghai Sixth People's Hospital Affiliated to Shanghai Jiao Tong University School of Medicine, Shanghai, China
[2]Shanghai Key Laboratory of Orthopedic Implants, Department of Orthopedic Surgery, Shanghai Ninth People's Hospital, Shanghai Jiao Tong University School of Medicine, Shanghai, China
[3]Department of Bone and Joint Surgery, Department of Orthopedics, Renji Hospital, School of Medicine, Shanghai Jiaotong University, Shanghai 200127, China

Received: 9 May 2024 / Accepted: 12 February 2025
Published online: 18 February 2025

References

1. Gala L, Clohisy JC, Beaulé PE. Hip dysplasia in the Young Adult. J Bone Joint Surg Am. 2016;98(1):63–73.
2. Zhang S, Doudoulakis KJ, Khurwal A, Sarraf KM. Developmental dysplasia of the hip. Br J Hosp Med (Lond). 2020;81(7):1–8.
3. Luo S, Kong L, Wang J, Nie H, Luan B, Li G. Development of modified Ilizarov hip reconstruction surgery for hip dysfunction treatment in adolescent and young adults. J Orthop Translat. 2021;27:90–5.
4. Zhen G, Guo Q, Li Y, Wu C, Zhu S, Wang R, Guo XE, Kim BC, Huang J, Hu Y, et al. Mechanical stress determines the configuration of TGFβ activation in articular cartilage. Nat Commun. 2021;12(1):1706.
5. Zhang H, Bei M, Zheng Z, Liu N, Cao X, Xiao Y, Lian Q, Wang Y, Hou X, Tian F. Parathyroid hormone (1–34) attenuates cartilage degradation and preserves subchondral bone micro-architecture in rats with Patella Baja-Induced-Patellofemoral Joint Osteoarthritis. Calcif Tissue Int. 2022;111(1):87–95.
6. Fang CL, Liu B, Wan M. Bone-SASP in skeletal aging. Calcif Tissue Int. 2023;113(1):68–82.
7. Zhen G, Cao X. Targeting TGFβ signaling in subchondral bone and articular cartilage homeostasis. Trends Pharmacol Sci. 2014;35(5):227–36.
8. Nicogossian A. Medicine and space exploration. Lancet. 2003;362:s8–9.
9. Ye T, Xue F, Hu H, He Z, Wang M, Yu Z, Zhao B, Chu L. Early emergent and progressive aberrant subchondral bone remodeling coupled with aggravated cartilage degeneration in Developmental Dysplasia of the hip. Cartilage. 2022;13(2):19476035221098165.
10. Chu L, He Z, Qu X, Liu X, Zhang W, Zhang S, Han X, Yan M, Xu Q, Zhang S, et al. Different subchondral trabecular bone microstructure and biomechanical properties between developmental dysplasia of the hip and primary osteoarthritis. J Orthop Translat. 2020;22:50–7.
11. You L, Temiyasathit S, Lee P, Kim CH, Tummala P, Yao W, Kingery W, Malone AM, Kwon RY, Jacobs CR. Osteocytes as mechanosensors in the inhibition of bone resorption due to mechanical loading. Bone. 2008;42(1):172–9.
12. Fillingham Y. J Jacobs 2016 Bone grafts and their substitutes. Bone Joint J 98-b 1 Suppl A 6–9.
13. Wang L, You X, Zhang L, Zhang C, Zou W. Mechanical regulation of bone remodeling. Bone Res. 2022;10(1):16.
14. Qing H, Ardeshirpour L, Pajevic PD, Dusevich V, Jähn K, Kato S, Wysolmerski J, Bonewald LF. Demonstration of osteocytic perilacunar/canalicular remodeling in mice during lactation. J Bone Min Res. 2012;27(5):1018–29.
15. Tang SY, Herber RP, Ho SP, Alliston T. Matrix metalloproteinase-13 is required for osteocytic perilacunar remodeling and maintains bone fracture resistance. J Bone Min Res. 2012;27(9):1936–50.
16. Yee CS, Schurman CA, White CR, Alliston T. Investigating Osteocytic Perilacunar/Canalicular remodeling. Curr Osteoporos Rep. 2019;17(4):157–68.
17. Bonewald LF. Generation and function of osteocyte dendritic processes. J Musculoskelet Neuronal Interact. 2005;5(4):321–4.
18. Mazur CM, Woo JJ, Yee CS, Fields AJ, Acevedo C, Bailey KN, Kaya S, Fowler TW, Lotz JC, Dang A, et al. Osteocyte dysfunction promotes osteoarthritis through MMP13-dependent suppression of subchondral bone homeostasis. Bone Res. 2019;7:34.
19. Tokarz D, Martins JS, Petit ET, Lin CP, Demay MB, Liu ES. Hormonal regulation of Osteocyte Perilacunar and Canalicular Remodeling in the Hyp Mouse Model of X-Linked Hypophosphatemia. J Bone Min Res. 2018;33(3):499–509.
20. Zhang H, Shao Y, Yao Z, Liu L, Zhang H, Yin J, Xie H, Li K, Lai P, Zeng H, et al. Mechanical overloading promotes chondrocyte senescence and osteoarthritis development through downregulating FBXW7. Ann Rheum Dis. 2022;81(5):676–86.
21. Singh M, Nagrath AR, Maini PS. Changes in trabecular pattern of the upper end of the femur as an index of osteoporosis. J Bone Joint Surg Am. 1970;52(3):457–67.
22. Perilli E, Baleani M, Ohman C, Baruffaldi F, Viceconti M. Structural parameters and mechanical strength of cancellous bone in the femoral head in osteoarthritis do not depend on age. Bone. 2007;41(5):760–8.
23. Macneil JA, Boyd SK. Bone strength at the distal radius can be estimated from high-resolution peripheral quantitative computed tomography and the finite element method. Bone. 2008;42(6):1203–13.
24. Ploton D, Menager M, Jeannesson P, Himber G, Pigeon F, Adnet JJ. Improvement in the staining and in the visualization of the argyrophilic proteins of the nucleolar organizer region at the optical level. Histochem J. 1986;18(1):5–14.
25. Montes GS, Junqueira LC. The use of the Picrosirius-polarization method for the study of the biopathology of collagen. Mem Inst Oswaldo Cruz. 1991;86(Suppl 3):1–11.
26. Rezakhaniha R, Agianniotis A, Schrauwen JT, Griffa A, Sage D, Bouten CV, van de Vosse FN, Unser M, Stergiopulos N. Experimental investigation of collagen waviness and orientation in the arterial adventitia using confocal laser scanning microscopy. Biomech Model Mechanobiol. 2012;11(3–4):461–73.
27. Muratovic D, Findlay DM, Quarrington RD, Cao X, Solomon LB, Atkins GJ, Kuliwaba JS. Elevated levels of active transforming growth factor β1 in the subchondral bone relate spatially to cartilage loss and impaired bone quality in human knee osteoarthritis. Osteoarthritis Cartilage. 2022;30(6):896–907.
28. Han X, Cui J, Chu L, Zhang W, Xie K, Jiang X, He Z, Du J, Ai S, Sun Q, et al. Abnormal subchondral trabecular bone remodeling in knee osteoarthritis under the influence of knee alignment. Osteoarthritis Cartilage. 2022;30(1):100–9.
29. Chu L, Liu X, He Z, Han X, Yan M, Qu X, Li X, Yu Z. Articular cartilage degradation and aberrant subchondral bone remodeling in patients with osteoarthritis and osteoporosis. J Bone Min Res. 2020;35(3):505–15.
30. He Z, Li H, Han X, Zhou F, Du J, Yang Y, Xu Q, Zhang S, Zhang S, Zhao N, et al. Irisin inhibits osteocyte apoptosis by activating the Erk signaling pathway in vitro and attenuates ALCT-induced osteoarthritis in mice. Bone. 2020;141:115573.
31. Vijayan V, Gupta S. Role of osteocytes in mediating bone mineralization during hyperhomocysteinemia. J Endocrinol. 2017;233(3):243–55.
32. Kerschnitzki M, Wagermaier W, Roschger P, Seto J, Shahar R, Duda GN, Mundlos S, Fratzl P. The organization of the osteocyte network mirrors the extracellular matrix orientation in bone. J Struct Biol. 2011;173(2):303–11.
33. Hu W, Chen Y, Dou C, Dong S. Microenvironment in subchondral bone: predominant regulator for the treatment of osteoarthritis. Ann Rheum Dis. 2021;80(4):413–22.
34. Goldring SR, Goldring MB. Changes in the osteochondral unit during osteoarthritis: structure, function and cartilage-bone crosstalk. Nat Rev Rheumatol. 2016;12(11):632–44.
35. Sanchez C, Deberg MA, Piccardi N, Msika P, Reginster JY, Henrotin YE. Subchondral bone osteoblasts induce phenotypic changes in human osteoarthritic chondrocytes. Osteoarthritis Cartilage. 2005;13(11):988–97.
36. Liu J, Wu X, Lu J, Huang G, Dang L, Zhang H, Zhong C, Zhang Z, Li D, Li F, et al. Exosomal transfer of osteoclast-derived miRNAs to chondrocytes contributes to osteoarthritis progression. Nat Aging. 2021;1(4):368–84.
37. Ni GX, Zhan LQ, Gao MQ, Lei L, Zhou YZ, Pan YX. Matrix metalloproteinase-3 inhibitor retards treadmill running-induced cartilage degradation in rats. Arthritis Res Ther. 2011;13(6):R192.
38. Sanchez C, Deberg MA, Bellahcène A, Castronovo V, Msika P, Delcour JP, Crielaard JM, Henrotin YE. Phenotypic characterization of osteoblasts from the sclerotic zones of osteoarthritic subchondral bone. Arthritis Rheum. 2008;58(2):442–55.
39. Liu XH, Kirschenbaum A, Yao S, Levine AC. Interactive effect of interleukin-6 and prostaglandin E2 on osteoclastogenesis via the OPG/RANKL/RANK system. Ann N Y Acad Sci. 2006;1068:225–33.
40. Liu XH, Kirschenbaum A, Yao S, Levine AC. Cross-talk between the interleukin-6 and prostaglandin E(2) signaling systems results in enhancement of osteoclastogenesis through effects on the osteoprotegerin/receptor activator of nuclear factor-{kappa}B (RANK) ligand/RANK system. Endocrinology. 2005;146(4):1991–8.

41. Lee SE, Woo KM, Kim SY, Kim HM, Kwack K, Lee ZH, Kim HH. The phosphatidylinositol 3-kinase, p38, and extracellular signal-regulated kinase pathways are involved in osteoclast differentiation. Bone. 2002;30(1):71–7.
42. Plotkin LI, Gortazar AR, Davis HM, Condon KW, Gabilondo H, Maycas M, Allen MR, Bellido T. Inhibition of osteocyte apoptosis prevents the increase in osteocytic receptor activator of nuclear factor κB ligand (RANKL) but does not stop bone resorption or the loss of bone induced by unloading. J Biol Chem. 2015;290(31):18934–42.
43. Cabahug-Zuckerman P, Frikha-Benayed D, Majeska RJ, Tuthill A, Yakar S, Judex S, Schaffler MB. Osteocyte apoptosis caused by Hindlimb Unloading is required to trigger osteocyte RANKL production and subsequent resorption of cortical and trabecular bone in mice femurs. J Bone Min Res. 2016;31(7):1356–65.
44. Meakin LB, Galea GL, Sugiyama T, Lanyon LE, Price JS. Age-related impairment of bones' adaptive response to loading in mice is associated with sex-related deficiencies in osteoblasts but no change in osteocytes. J Bone Min Res. 2014;29(8):1859–71.
45. Klein-Nulend J, Bacabac RG, Bakker AD. Mechanical loading and how it affects bone cells: the role of the osteocyte cytoskeleton in maintaining our skeleton. Eur Cell Mater. 2012;24:278–91.
46. Klein-Nulend J, Bakker AD, Bacabac RG, Vatsa A, Weinbaum S. Mechanosensation and transduction in osteocytes. Bone. 2013;54(2):182–90.
47. Kroker A, Zhu Y, Manske SL, Barber R, Mohtadi N, Boyd SK. Quantitative in vivo assessment of bone microarchitecture in the human knee using HR-pQCT. Bone. 2017;97:43–8.

Publisher's note